Comparing Parameter Identification Strategies for a Saturated Model of an Induction Motor

A. Millán, C. Villanueva
Departamento de Electrónica y Comunicaciones
Universidad de Carabobo
Valencia, Venezuela
ajmillan@uc.edu.ve

J. Restrepo, J. Aller, V. Guzmán, M. Giménez, J. Viola
Grupo de Sistemas Industriales de Electrónica de Potencia
Universidad Simón Bolívar
Caracas, Venezuela
restrepo@usb.ve

***Abstract*—Parameter identification for the dynamic model of an induction motor is evaluated, taking into account the magnetic saturation curve. The identification scheme is based on a Particle Swarm Optimization algorithm to fit the motor and model startup stator currents curves. Two different strategies are compared. The first one adds the saturation effects on the magnetizing inductance after using a linear inductance model in the identification process; the second one includes the magnetic saturation curve through the model identification process. The resultant models are tested in a variable flux motor control system. Results show differences in the dynamic response for the magnetizing current.**

***Keywords*-Induction Motor; Parameter Identification; Saturated Model**

I. Introduction

The need for accurate and efficient control of induction motor motivated the development of dynamic models to adequately represent their behavior in both steady state and transient operation [1]-[2]. Most of these are parametric models with a structure that derives from physical laws and principles of motor operation and whose parameters values are inferred from measurement data.

The study of the dependence of parameter values to the magnitude of the magnetization flux is justified in motor control systems operating at variable flux levels, which are motivated by applications that require: Increase in torque demand with reduced current consumption and/or improvement in the energy efficiency of the control process.

In a first approximation, the parameters values for the classical model of the induction motor can be obtained using various methods that assume a linear magnetic circuit for the flux [3]-[5], which is valid in applications where the motor operates with a constant flux rate. However, when the motor works in situations that require significant changes of flux, the actual magnetic saturation curve of the motor changes the magnitude of the inductive coupling between its windings, which modifies the parameters values, degrading the performance of the controllers based on linear parametric models for estimation of the control variables.

Several models have been developed to include the saturation effects in the induction motor [6]-[10]. From these models is possible to improve the representation of the behavior of the induction motor. However, the knowledge of the magnetization characteristic must be incorporated into the model and the parameters values must be properly identified.

A widespread strategy is to identify the model parameters from data of the startup stator current curve, while considering constant the magnetizing inductance [11]-[13]. When the model is used in variable flux applications, the inductance is adjusted according to data from the magnetization curve of the motor.

This work includes the characteristic curve of magnetization through the model identification process, which complicates the problem, but provides better results for the parameters nondependent on the flux level. The technique of Particle Swarm Optimization is used to minimize the error between the model output and the measured data from the motor, in order to solve the convergence problems presented by other methods, such as those based on gradients, given the nonlinear characteristic of the induction motor.

II. Induction Motor

A. Flux Model

In this case flux links are used as state variables to solve the model, thereby avoiding the numerical calculation of flux derivatives.

$$\frac{d\vec{\lambda}_e}{dt} = \vec{v}_e - R_e\vec{i}_e \tag{1}$$

$$\frac{d\vec{\lambda}_r}{dt} = -R_r\vec{i}_r + j\cdot\omega_r\vec{\lambda}_r \tag{2}$$

$$\vec{i}_e = \frac{L_e\vec{\lambda}_e - L_m\vec{\lambda}_r}{L_eL_r - {L_m}^2} = i_{ed} + j\cdot i_{eq} \tag{3}$$

$$\vec{i}_r = \frac{L_r\vec{\lambda}_r - L_m\vec{\lambda}_e}{L_eL_r - {L_m}^2} = i_{rd} + j\cdot i_{rq} \tag{4}$$

where $\vec{v}_e$, $\vec{\lambda}_e$, $\vec{\lambda}_r$, $\vec{i}_e$ and $\vec{i}_r$ are space vectors for stator voltage, stator flux, rotor flux, stator current and rotor current referred to the stator stationary coordinates; R_e and L_e are

978-0-7695-4882-1/12 $26.00 © 2012 IEEE
DOI 10.1109/Andescon.2012.37

the stator windings's resistance and inductance, R_r and L_r are the rotor windings's resistance and inductance, L_m is the magnetizing inductance and ω_r is the angular velocity of the rotor.

B. Flux Model including Saturation

From the resulting currents in (3) and (4), the magnitude of the magnetizing flux is calculated by (5). Then the magnetizing current is determined using a function $f(\lambda_m)$ which describes the actual magnetization characteristic of the motor. Finally L_m gets through (6).

$$\lambda_m = L_m \sqrt{(i_{ed} + i_{rd})^2 + (i_{eq} + i_{rq})^2} \tag{5}$$

$$L_m(\lambda_m) = \frac{\lambda_m}{i_m} = \frac{\lambda_m}{f(\lambda_m)} \tag{6}$$

The magnetizing inductance is updated following the diagram presented in Fig. 1.

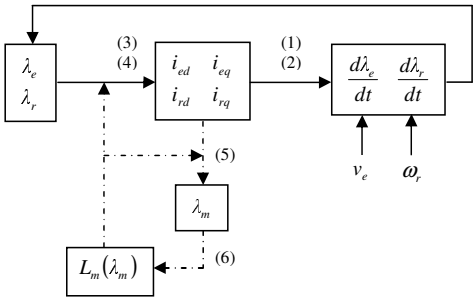

Figure 1. Diagram for the solution of the dynamic model of the induction motor, using flux links as state variables.

III. Parameter Identification

A. Scheme for Model Parameters Identification

The scheme used to identify the model parameters vector $\hat{\boldsymbol{\theta}}_k$, defined as in (7), is presented in Fig. 2. In the scheme, $\boldsymbol{y}_k$ and $\hat{\boldsymbol{y}}_k$ are the outputs measured from the real system and from the model, for the same input $\boldsymbol{u}_k$.

$$\hat{\boldsymbol{\theta}}_k = \left[\hat{R}_{e,k} \quad \hat{R}_{r,k} \quad \hat{L}_{m,k} \quad \hat{L}_{e,k} \quad \hat{L}_{r,k}\right] \tag{7}$$

Model quality is evaluated in terms of the error $\boldsymbol{e}_k = \boldsymbol{y}_k - \hat{\boldsymbol{y}}_k$. Then, the values of the model parameters vector must be properly adjusted to minimize the error, which is done according to the identification algorithm method.

Instead of the error, a quadratic function of the error is selected to ensure the existence of a global minimum (8).

$$h\left(\hat{\boldsymbol{\theta}}_k\right) = \boldsymbol{e}_k^T \boldsymbol{e}_k \tag{8}$$

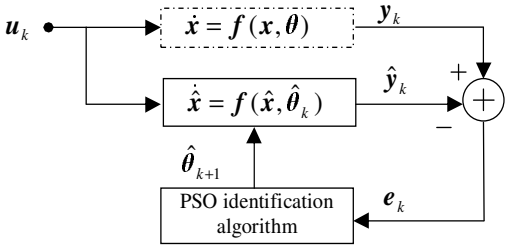

Figure 2. Model parameters identification scheme using PSO algorithm.

B. PSO Identification Algorithm

The Particle Swarm Optimization is a technique based on artificial intelligence, inspired in the Swarms Theory, developed by Kennedy and Eberhart in 1995 [14].

PSO uses a population of M particles or agents, each one representing a potential solution to the optimization problem. These agents move randomly in the N-dimensional space defined by the degrees of freedom of the problem, searching for an optimal solution.

In general terms, the velocity vector $\boldsymbol{v}_{k+1}^m$ of the m-agent is determined stochastically according to the distance between its current position $\hat{\boldsymbol{\theta}}_k^m$, the best personal position $\hat{\boldsymbol{\theta}}_{pbest}^m$ and the best collective position $\hat{\boldsymbol{\theta}}_{gbest}$. These conditions can be written in simplified form (9).

$$\begin{aligned} \boldsymbol{v}_{k+1}^m = w \cdot \boldsymbol{v}_k^m + c_1 \cdot r_{1,k} \left(\hat{\boldsymbol{\theta}}_{pbest}^m - \hat{\boldsymbol{\theta}}_k^m\right) + \ldots \\ + c_2 \cdot r_{2,k} \left(\hat{\boldsymbol{\theta}}_{gbest} - \hat{\boldsymbol{\theta}}_k^m\right) \\ for \quad m = 1, 2, \ldots M \end{aligned} \tag{9}$$

r_1 y r_2 are normally distributed random numbers between [0,1], w is used to incorporate a moment of inertia to the system, while c_1 and c_2 are used to weigh up the personal and collective knowledge and must be adjusted to tune the swarm, typically $c_1 = c_2 = 1$. The agents move to a new position for the next iteration according to the velocity vector obtained, using (10). The adjustment coefficient η_k is used to accelerate the convergence of the solution, in most cases $\eta_k = 1$.

$$\hat{\boldsymbol{\theta}}_{k+1}^m = \hat{\boldsymbol{\theta}}_k^m + \eta_k \cdot \boldsymbol{v}_{k+1}^m \tag{10}$$

IV. Experimental Results

A. Induction Motor

The data set used to compare simulation strategies was acquired from a 1HP Siemens motor, model 1LA7080-4YA60, 220 V / 3.5 A.

Stator voltages, and currents presented in Fig. 3(a), were recorded during a start-up test, at nominal line voltage and no load. For each of the variables 2.500 samples were recorded (L=2.500), acquired at a 10kHz sampling frequency.

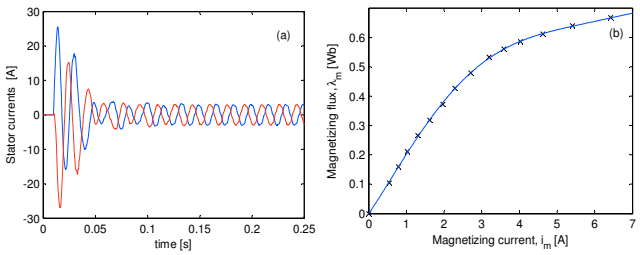

Figure 3. Experimental data. a) startup stator currents. b) magnetizing flux-current curve.

The magnetizing characteristic curve, plotted in Fig. 3(b), was calculated from stator voltage and current measurements performed with the motor running in steady state, for supply voltage set within the range of 0.2 to 1.15 times the nominal value.

B. Parameter Identification Results

The identification process was carried out according to the scheme of Fig. 2, using the previously recorded stator voltages and currents as $\boldsymbol{u}_k \boldsymbol{y}_k$ respectively.

The swarm for the PSO algorithm was configured with M=10 agents, $c_1 = 1.5$, $c_2 = 1.0$ and $w = 0.7$.

At each iteration k, equations (1)-(4) were solved for each m-agent and its parameters values adjusted according to (9)-(10), minimizing the magnitude of its mean squared error, where $\boldsymbol{e}_k^m = \boldsymbol{y}_k - \boldsymbol{y}_k^m$.

Two different approaches were used to build a saturated model to be tested in a variable flux motor control system.

1) Linear model identification: The identification process was carried out considering a constant magnetizing flux-current ratio, taking into account only the solid line path for solving the diagram in Fig. 1. After this, the final model uses the resultant resistance and dispersion parameters, incorporating the magnetizing characteristic to adjust L_m according to the flux level.

2) Saturated model identification: This approach includes the magnetic saturation curve information through the whole model identification process, and later use of the model, including the dotted line path for solving the diagram in Fig.1. The resultant estimated parameters values for both approaches are shown in Table I. In the error calculations the linear model was used as reference.

Table I
ESTIMATED PARAMETERS VALUES

Parameter	Linear	Saturated	Error
$\hat{R}_e$	3.07Ω	3.01Ω	-1.95%
$\hat{R}_r$	2.87Ω	3.06Ω	-6.62%
$\hat{L}_m$	$151.60mH$	N/A	N/A
$\hat{L}_{e\delta} + \hat{L}_{r\delta}$	$12.79mH$	$13.32mH$	4.14%
$h\left(\hat{\theta}_{gbest}\right)$	0.1788	0.1527	-14.59%

Fig. 4 shows how mean square error, stator and rotor resistances and total dispersion inductance values evolve in both identification processes after $k = 200$ iterations.

For both the linear model and the saturated models the algorithm converges to a first local minimum at approximately thirty iterations ($k = 30$), but the saturated model gives better overall results, with a 15% error reduction after eighty iterations ($k = 80$).

Stator resistance R_e converges to almost the same value for both schemes, with a difference of less than 2%, while the rotor resistance R_r and the total dispersion inductance $L_\delta = L_{e\delta} + L_{r\delta}$ are adjusted to higher values in the saturated model. These results are in agreement with results presented in [15] for a gradient-based identification process, using a parametric sensibility analysis for the same motor.

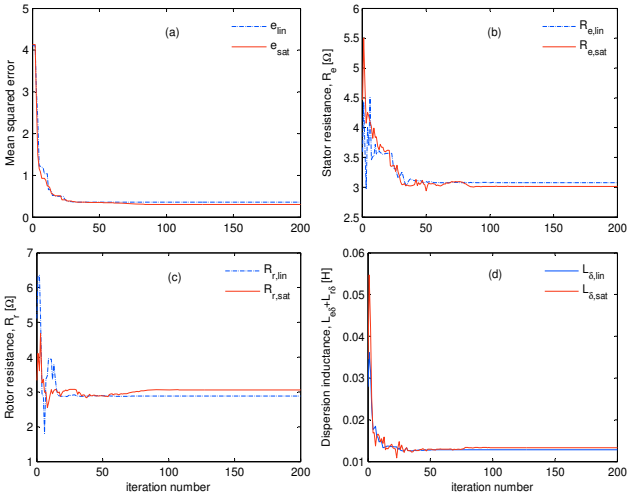

Figure 4. Identification process results. a) mean squared error. b) stator resistance. c) rotor resistance. d) total dispersion inductance.

C. Variable Flux Motor Control System

Both models were used for the simulation of a torque control system with variable flux level. The motor started loaded and the system was required to supply a constant torque of 2-Nm to the load.

As shown in Fig. 5 after the system stabilized, at time $t = 0.5s$ the reference signal for the direct axis current was changed from 4A to 2.5A. This action forces a change in the quadrature current reference in order to preserve the constant torque set point.

Similar in both cases, but as shown in Fig. 5(c) and 5(d), the magnetizing current and the torque transient responses are better in the saturated model, which produces faster convergence and less torque fluctuations.

These differences were also appreciated in the magnetizing current dynamic response, Fig. 6, in a vector control real implementation using a Dynamic Test System [16].

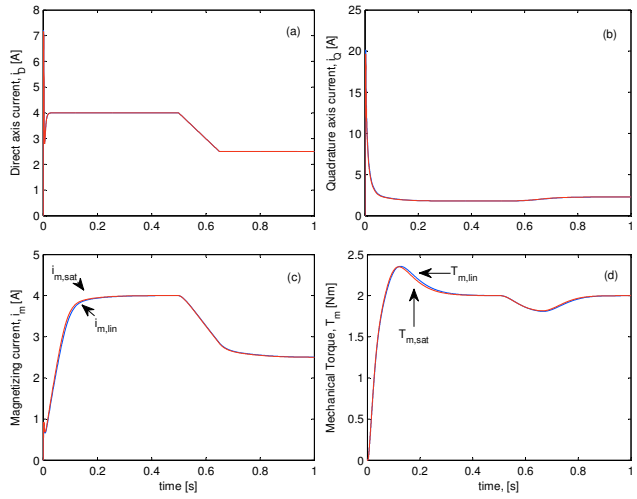

Figure 5. Vector control simulation results. a) direct axis current. b) quadrature axis current. c) magnetizing current. d) torque.

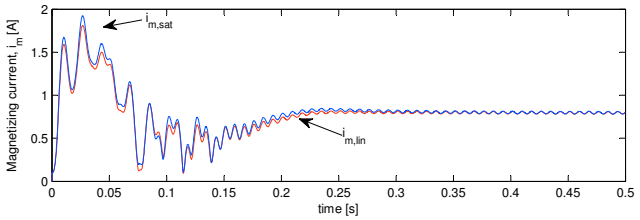

Figure 6. Experimental values measured for the magnetizing current on a vector control system using both models. $i_{m,lin}$:linear model. $i_{m,sat}$:saturated model.

V. Conclusion

Incorporating the magnetizing characteristic curve into the identification process improves the model performance for represent the motor dynamic behavior. This is important for applications that require changes in the flux level operating point, such as electric traction or when increasing energy efficiency.

Acknowledgment

The authors would like to thank the financial support granted by Fondo Nacional de Ciencia Tecnología e Innovación FONACIT, Strategic Projects Program 2011, and Consejo de Desarrollo Científico y Humanístico de la Universidad de Carabobo CDCH-UC, project CDCH-AM-0424-10.

References

[1] J. Bocker and S. Mathapati, *State of the Art of Induction Motor Control*, IEEE International Electric Machines & Drives Conference, IEMDC '07, vol. 2, pp 1459-1464, 2007.

[2] J. W. Finch and D. Giaouris, *Controlled AC Electrical Drives*, IEEE Transactions on Industrial Electronics, vol. 55, N. 2, pp 481-491, 2008.

[3] H. Toliyat, E. Levi and M. Raina, *A Review of RFO Induction Motor Parameter Estimation Techniques*, IEEE Transactions on Energy Conversion, vol. 18, N. 2, June 2003.

[4] K. S. Huang, Q. H. Wu and D. R. Turner, *Effective identification of induction motor parameters based on fewer measurements*, IEEE Transaction on Energy Conversion, vol.17, N. 1, pp 55 -60, 2002.

[5] F. Corcoles, J. Pedra, M. Salichs and L. Sainz, *Analysis of the induction machine parameter identification*, IEEE Transaction on Energy Conversion, vol. 17, N. 2, pp 183-190, 2002.

[6] T. A. Najafabadi and S. M. Nabavi, *The Analysis of Saturation and Coreloss Effects of Induction Motor Direct Starting*, Proceedings of International Conference on Electrical Machines and Systems, ICEMS 2007, pp 1265-1268, 2007.

[7] M. Beniakar, K. Pavlou and A. Kladas, *Nonlinear Induction Motor Control Accounting for Inductance Saturation*, Proceedings of International Conference on Electrical Machines, ICEM 2008, pp 1-4, 2008.

[8] E. V. N. Souza and S. R. Naidu, *Accurate Modeling of the Three Phase Induction Motor including Saturation Effects*, Proceedings of IEEE 5th International Conference on Power Electronics and Motion Control, IPEMC 2006, pp 1-5, 2006.

[9] J. C. Moreira and T. A. Lipo, *Modeling of Saturated ac Machines including Air Gap Flux Harmonic Components*, IEEE Transactions on Industry Applications, vol. 28, N. 2, March 1992.

[10] V. Donescu, A. Charette, Z. Yao and V. Rajagopalan, *Modeling and Simulation of Saturated Induction Motors in Phase Quantities*, IEEE Transactions on Energy Conversion, vol. 14, N. 3, September 1999.

[11] K. Wang, J. Chiasson, M. Bodson and L. M. Tolbert, *A nonlinear least-squares approach for identification of the induction motor parameters*, IEEE Trans. on Automatic Control, vol. 50, N. 10, pp 1622-1628, Oct. 2005.

[12] C. Picardi and N. Rogano, *Parameter identification of induction motor based on particle swarm optimization*, International Symposium on Power Electronics, Electric Drives, Automation and Motion, pp S132-S137, May 2006.

[13] C. Guangyi, G. Wei and H. Kaisheng, *On line parameter identification of an induction motor using improved particle swarm optimization*, Proceedings of the 26th Chinesse Control Conference, pp. 745-749, Jul. 2007

[14] J. Kennedy and R. Eberhart, *Particle Swarm Optimization*, Proceedings of the IEEE International Conference on Neural Networks, vol. 4, pp. 1942-1948, Nov.-Dic. 1995.

[15] A. Millán, *Efectos de la Saturación magnética en la Identificación de Parámetros del Modelo Dinámico del Motor de Inducción*, Trabajo de Ascenso a la Categoría de Profesor Titular, Universidad de Carabobo, Valencia, Venezuela, 2012.

[16] M. Giménez et al., *Plataforma: Development of an Integrated Dynamic Test System to determine Power Electronics Systems Performance*, Revista de la Facultad de Ingeniería de la UCV, Caracas, Venezuela, vol. 23, N. 3, pp 91-102, 2008.